

# Effect of Electrolytes on the Catalytic Properties and Structural Characteristics of Dodecylpyridinium Bromide Micelles

L. Ya. Zakharova, D. B. Kudryavtsev, L. A. Kudryavtseva, Yu. F. Zuev,  
N. L. Zakharchenko, N. N. Vylegzhanina, Z. Sh. Idiyatullin, and V. D. Fedotov

Arbuzov Institute of Organic and Physical Chemistry, Kazan Research Center,  
Russian Academy of Sciences, Kazan, Tatarstan, Russia

Kazan State University of Technology, Kazan, Tatarstan, Russia

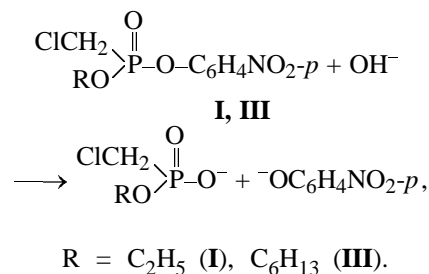
Institute of Biochemistry and Biophysics, Kazan Research Center,  
Russian Academy of Sciences, Kazan, Tatarstan, Russia

Received March 16, 2000

**Abstract**—Electrolyte-induced structural rearrangements of dodecylpyridinium bromide micelles affect their catalytic properties in alkaline hydrolysis of phosphonic esters.

Even though the effect of electrolytes on the catalytic properties of ionic micelles is being extensively studied [1–3], some essential aspects of this problem still remain unexplored. Of them, the most interesting one seems to be the influence of salt-induced structural rearrangements of micelles on the micellar effect. It is known [4–6] that electrolytes affect many properties of ionic micelles, reducing the critical concentration of micelle formation ( $c_{\text{CCM}}$ ), increasing the aggregation number and the degree of bonding of counterions, and changing the form of aggregates. At a certain critical concentration of electrolytes, the smooth change in the above characteristics gives way to a sharp, jumpwise one, which is analytically detected by an inflection in property–salt concentration logarithm plots. According to [4], these threshold concentrations of electrolytes correspond to a *sphere–cylinder* micellar transformation. It appears reasonable to propose that changes in the above structural characteristics can affect the reactivity of compounds in micelles. It is this aspect of the salt effect which is the principal subject of the present investigation. We earlier studied [7, 8] the nature of the effect of electrolytes on the rate of alkaline hydrolysis and acid–base equilibria in cetyltrimethylammonium and cetylpyridinium bromide micelles. Here we focused on the kinetics of alkaline hydrolysis of ethyl *p*-nitrophenyl chloromethylphosphonate (**I**) in a micellar solution of dodecylpyridinium bromide (**II**) over a wide range of KCl, KBr, and sodium salicylate (NaSal) concentrations. To compare the electrolyte effects on the kinetics of hydrolysis of compounds of different hydrophobicity, we also studied alkaline hydrolysis of hexyl *p*-nitrophenyl chloromethylphos-

phonate (**III**) in the presence of sodium salicylate. By surface tension measurements and ESR and  $^1\text{H}$  NMR spectroscopy we also studied the structural behavior of surfactant **II** micelles in the presence of the salicylate ion.



According to the pseudophase model of micellar catalysis [9], reagents (substrate with electrophilic center on the phosphorus atom and the hydroxide ion as nucleophilic agent) are distributed between the aqueous and micellar pseudophases. The solubilization of the reagents is measured by the binding constants of the substrate ( $K_{\text{S}}$ ,  $\text{l mol}^{-1}$ ) and the nucleophile ( $K_{\text{OH}}$ ,  $\text{l mol}^{-1}$ ) to micelles. The reaction proceeds in both pseudophases and is characterized by second-order rate constants [ $k_{2,\text{w}}$ ,  $\text{l mol}^{-1} \text{s}^{-1}$  and  $k_{2,\text{m}}$ ,  $\text{l mol}^{-1} \text{s}^{-1}$ , for the aqueous and micellar phases, respectively]. The kinetic data were treated as described in [10, 11]. The pseudophase model recognizes two main factors determining the micellar effect, namely, the concentration ( $F_{\text{c}}$ ) and micellar microenvironment ( $F_{\text{m}}$ ) factors (see table). The  $F_{\text{m}}$  value characterizes the change in the reaction rate, produced by reagent transfer from bulk pseudophase into micellar and by changes in reagent microenvironment

Results of quantitative analysis of kinetic data (Fig. 1) in terms of the pseudophase model

$c_{\text{salt}},$ M	$k_{2,m},$ $\text{l mol}^{-1} \text{s}^{-1}$	$K_S,$ $\text{l mol}^{-1}$	$K_{\text{OH}},$ $\text{l mol}^{-1}$	$F_c$	$F_m$	$(k_{\text{app}}/k_w)_{\text{max}}$	$F_c F_m$
NaSal (for <b>I</b> )							
0	11.7	233	1.4	3.9	2.9	10.4	11.5
0.005	5.0	200	3.0	7.9	1.3	8.6	9.8
0.01	4.5	83	3.0	7.0	1.1	7.0	8.0
0.02	1.1	63	11.0	19.0	0.3	4.0	5.0
NaSal (for <b>III</b> )							
0	0.9	527	24	55.0	0.36	20.0	19.7
0.005	12.8	511	0.64	2.0	5.13	10.0	10.0
KBr (for <b>I</b> )							
0.01	4.6	60	3.3	7.3	1.2	7.6	8.4
0.02	1.7	100	6.9	14.3	0.43	5.2	6.2
0.08	1.0	48	12.0	17.8	0.3	3.1	4.6
KCl (for <b>I</b> )							
0.02	5.0	190	2.4	6.5	1.3	7.5	8.5
0.03	2.5	250	3.9	10.0	0.6	5.5	6.6
0.08	1.6	215	5.3	13.3	0.4	4.1	5.4
0.2	0.8	95	12.3	22.1	0.2	3.0	4.0

(micropolarity, solvation shell, etc.). The parameter  $F_c$  describes the catalytic effect resulting from the local increase in the concentrations of the reagents on their solubilization in the micellar pseudophase which has a much smaller volume than the solvent pseudophase.

Figures 1–3 represent the kinetic data, and the table lists the results of quantitative analysis of the experimental  $k_{\text{app}}-c_{\text{II}}$  dependences. Comparison of the data in Figs. 1 and 2 shows that the kinetics of hydrolysis of substrates **I** and **III** are described by kinetic curves of different shapes. The presence of saturation (Fig. 1) is indicative of a poor solubilization of substrate **I** by surfactant **II** micelles ( $K_S$  233  $\text{l mol}^{-1}$ ). The catalytic effect  $[(k_{\text{app}}/k_w)]_{\text{max}}$  is ca. 10) is determined by positive contributions of the concentration ( $F_c$  3.9) and micellar microenvironment ( $F_m$  2.9) factors. The observation of a maximum in the kinetic curve for phosphonate **III** results from effective binding of the substrate ( $K_S$  527  $\text{l mol}^{-1}$ ) in the range of relatively low concentrations of surfactant **II**. Thus, further raising the concentration of micelles leads to dilution of the reagents and weakens the concentration effect. The catalytic effect  $[(k_{\text{app}}/k_w)]_{\text{max}}$  ca. 20) in this case is determined by a positive contribution of the concentration factor ( $F_c$  55), while micellar environment adversely affects the reaction rate ( $F_m$  0.36).

In the presence of electrolytes the apparent rate constant is decreased. The inhibiting effect (salt effect) is to a great extent dependent on the nature of the counterion and decreases in the order  $\text{Sal}^- \gg$

$\text{Br}^- > \text{Cl}^-$ . According to the pseudophase model [9], one of the possible reasons for such inhibition may lie in decrease in the surface potential of micelles with increasing counterion concentration. This results in weakened electrostatic attraction of the hydroxide ions to the positively charged surface of micelles, where the reaction takes place. An alternative mechanism of inhibition can be connected with washing out the substrate from the Stern layer with increasing degree of counterion binding. Comparison of data for substrates **I** and **III** (see table) shows that, depending on the efficiency of the micellar catalysis and the nature of the reactants, both mechanisms of the salt effect can be operative. In the case of the weakly hydrophobic substrate **I**, electrolytes decrease the binding constant of the substrate and the rate of the reaction in the micellar phase. The sharp decrease in  $K_S$  with increasing salt concentration indicates that the substrate is expelled from the micellar surface by counterions, i.e., the second mechanism of inhibition is operative. Similar effect is observed not only on addition of hydrophobic salicylate, but also in the presence of hydrophilic inorganic counterions (see table). As follows from the table, there is a compensating change in the concentration (increase) and micellar environment (decrease) factors for organic and inorganic counterions.

With the more hydrophobic substrate **III**, the kinetic curve changes shape, implying weakened catalysis and concentration effect. It is seen from the

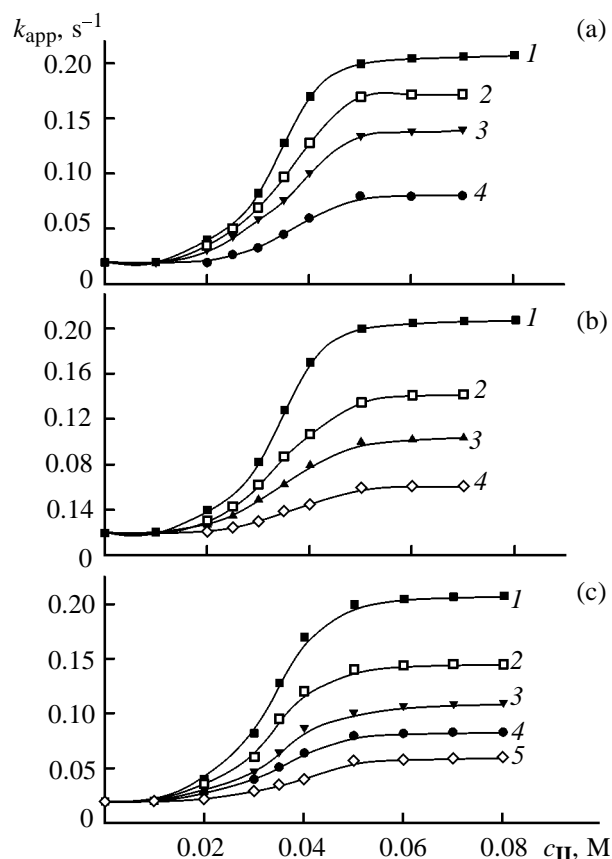


**Fig. 1.** Plots of the rate constants  $k_{app}$  of alkaline hydrolysis of substrate **I** in micellar solutions of compound **II** vs. the concentration of the latter ( $c_{NaOH}$  0.005 M, 25°C). (a)  $c_{NaSal}$ , M: (1) 0, (2) 0.005, (3) 0.01, and (4) 0.02. (b)  $c_{KBr}$ , M: (1) 0, (2) 0.01, (3) 0.02, and (4) 0.08. (c)  $c_{NaCl}$ , M: (1) 0, (2) 0.02, (3) 0.03, (4) 0.08, and (5) 0.2.

table, the  $K_{OH}$  value is strongly decreased in the presence of the  $Sal^-$  ions. Consequently, the first mechanism of inhibition is operative, associated with weakened electrostatic attraction of the hydroxide ions to the micellar surface because of decreased surface potential. In this case, too, compensating changes of the concentration and micellar microenvironment factors take place, but the tendency is opposite:  $F_c$  falls and  $F_m$  grows. A probable explanation for the different mechanisms of salt effects with compounds **I** and **III** is that the substrate changes localization as its hydrophobicity grows. Presumably, ester **I** is solubilized in the Stern layer of micelles, and, therefore, in the surface layer there is competition between the substrate and counterions. In this case, with increasing concentration of counterions, the substrate is expelled from the micellar phase and  $K_s$  decreases. The more hydrophobic phosphonate **III** is evidently

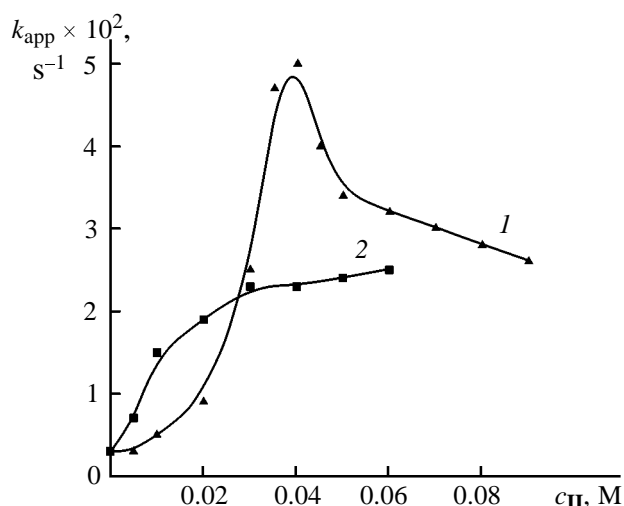


**Fig. 2.** Plots of the rate constants  $k_{app}$  of alkaline hydrolysis of substrate **III** in micellar solutions of compound **II** vs. the concentration of the latter ( $c_{NaOH}$  0.001 M, 25°C).  $c_{NaSal}$ , M: (1) 0 and (2) 0.005.

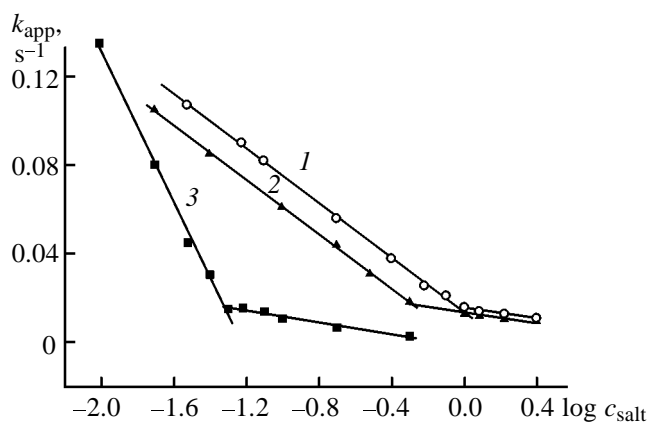


**Fig. 3.** Plots of the rate constants  $k_{app}$  of alkaline hydrolysis of substrate **I** in micellar solutions of compound **II** vs. the logarithm of salt concentration ( $c_{NaOH}$  0.005 M, 25°C). Salt: (1) KCl, (2) KBr, and (3) NaSal.

solubilized in the micelle core nearby the surface layer, thus not competing with counterions in the Stern layer. Here, increasing concentration of the unreactive counterions gives rise to expulsion of the highly hydrophilic hydroxide ions from the micellar surface and  $K_{OH}$  decreases.

In line with the aim of our study, we examined the kinetic data (Fig. 3) and established the critical concentrations of electrolytes ( $c_{cr}$ ), corresponding to the inflections in the  $k_{app}$ - $\log c_{salt}$  plots. According to [7, 8],  $c_{cr}$  values can be related to structural trans-

formations of surfactant **II** micelles. The  $c_{cr}$  values are 1.1, 0.5, and 0.05 M for  $Cl^-$ ,  $Br^-$ , and  $Sal^-$ , respectively.

To verify the proposed interrelationship between the structure of the micelles and the reactivity of the esters, we studied the properties of micellar solutions of surfactant **II** in the presence of electrolytes by means of surface tension measurements and ESR and  $^1H$  NMR spectroscopy. By surface tension measurements we found  $c_{CCM}$  values for solutions of compound **II** at various salt concentrations, and, basing on data in [6], deduced the following empirical relationships.

$$\log c_{CCM} = -0.41 \log c_{KCl} - 4.15,$$

$$\log c_{CCM} = -0.51 \log c_{KBr} - 2.87,$$

$$\log c_{CCM} = -0.85 \log c_{NaSal} - 5.32.$$

Analysis of the surface tension isotherms by the method proposed in [12] allowed us to estimate the degree of counterion binding ( $\beta$ ) at various concentrations of the  $Sal^-$  ions. It was shown that the degree of counterion binding sharply increases when the bromide ions on the surface of micelles are replaced by  $Sal^-$  ions. Given are  $c_{NaSal}$  (M) and  $\beta$ : 0, 0.71; 0.005, 0.92; 0.01, 0.94; and 0.08, 0.96.

Using the Nernst relationship between the surface potential ( $\Psi$ ) and  $c_{CCM}$ :  $d|\Psi|/d\log c_{CCM} = 59.16$  mV [13], we estimated the surface potential of compound **II** micelles at various electrolyte concentrations. The results are given in Fig. 4. As in [8], we found that the  $\Psi$  values corresponding to the critical concentrations of the  $Cl^-$  and  $Br^-$  ions are close to each other: 74 and 71 mV. This result points to prevailing contribution of the surface potential into the mechanism of the inhibiting effect of inorganic counterions on the reaction rates in micelles. The  $c_{cr}$  value for the  $Sal^-$  ions is  $-7$  mV. These results are not in conflict with literature, where negative values of the surface potential  $\Psi$  [14] and the electrokinetic  $\xi$  potential [15, 16] of cationic micelles in the presence of NaSal have been reported. The unique effect of the  $Sal^-$  ion on cetyltrimethylammonium bromide, cetylpyridinium bromide, and trimethyltetradecyl halide micelles, which differs from that of hydrophilic inorganic counterions, has been extensively studied in recent years [15, 16]. The behavior of surfactant **II** micelles in the presence of  $Sal^-$  ion has scarcely been studied. We investigated the effect of this counterion on the structure of compound **II** micelles.

The size and shape of the micelles were calculated basing on the self-diffusion coefficient of surfactant **II** ( $D$ ), measured by the diffusion decay of its  $(CH_2)_n$

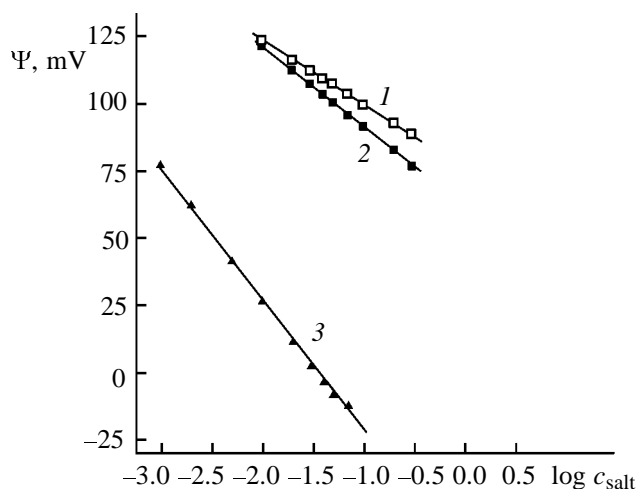


**Fig. 4.** Plots of the micellar surface potential of compound **II** vs. the logarithm of salt concentration. Salt: (1) KCl, (2) KBr, and (3) NaSal.

proton signals in the  $^1H$  NMR spectrum [17]. Given are  $c_{NaSal}$  (M) and  $D \times 10^{11}$  ( $m^2 s^{-1}$ ): 0, 14.0; 0.01, 11.4; 0.03, 6.21; 0.05, 2.00; 0.1, 1.38; and 0.2, 1.04. The effective radius of the micelles ( $R$ ), estimated by the Stokes–Einstein equation (1) from the diffusion data in the absence of NaSal, is 15.4 Å. This value is close to our estimate for the length of the molecule of surfactant **II** from bond lengths and angles (15.5 Å) and may suggest a spherical shape of the micelles.

$$D = kT/6\pi\eta R. \quad (1)$$

Here  $\eta$  is the viscosity of the solvent.

At higher concentrations of NaSal in the solution, the estimates for  $R$  by Eq. (1) are much larger than the hydrocarbon chain length in surfactant **II**, which does not agree with the assumed spherical shape of the micelles and probably results from their asymmetrization. Approximating the micelle by a stretched rotation ellipsoid and using the  $D$  values, we can obtain the micelle axis ratio ( $P$ ) [18]. As seen from Fig. 5, as the concentration of counterions is increased, the micelles change their shape, first from spherical to spherical-cylindrical ( $P$  1–5), and in the NaSal concentration region of 0.03–0.05 M, to cylindrical.

The shape of micelles is conveniently elucidated by investigating the mobility of spin labels by ESR spectroscopy [19]. The almost water-insoluble doxylstearic acids are liable to insert into micellar aggregates so that the mobility of the spin label bound to the  $C^5$  atom of the stearic acid will characterize the density of packing of surfactant molecules near polar head groups of micelles. Since spherical aggregates

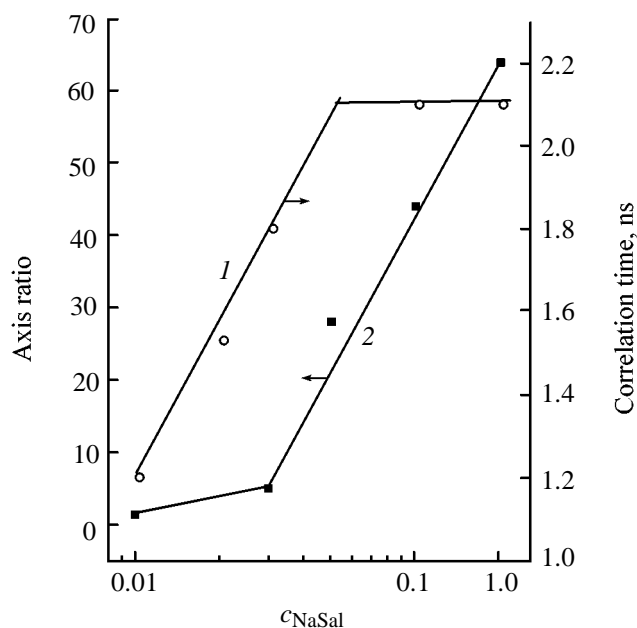


**Fig. 5.** Plots of (1) the correlation time of spin label rotation (in the absence of NaSal,  $\tau$  1.1 ns) and (2) surfactant **II** micelle axis ratio vs. NaSal concentration.

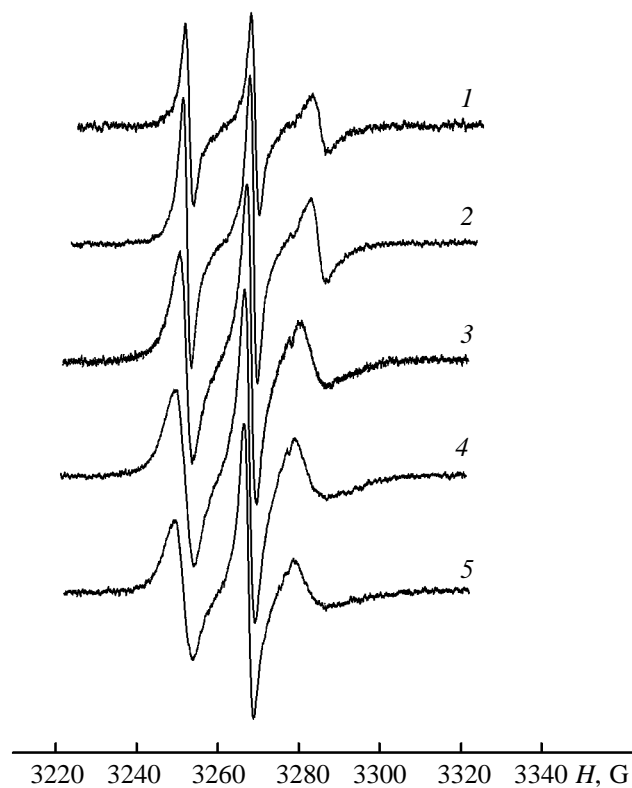


**Fig. 6.** ESR spectra of 5-doxylstearic acid in micellar solutions of surfactant **II**.  $c_{\text{NaSal}}$ , M: (1) 0, (2) 0.01, (3) 0.025, (4) 0.1, and (5) 0.4.

have a stronger surface curvature than cylindrical ones, they will feature a looser packing of surfactant molecules, thus making the spin label more mobile. Therefore, cylindrical micelles are characterized by longer correlation times of label rotation ( $\tau$ , s), as determined by Eq. (2).

$$\tau = 6.65\Delta H_+[(I_+/I_-)^{-1/2} - 1] \times 10^{-10}. \quad (2)$$

Here  $\Delta H_+$  is the width of the low-field hyperfine component in the ESR spectrum,  $I_+$  and  $I_-$  are the intensities of the low- and high-field hyperfine components, respectively. From the above it follows that the *sphere-cylinder* transition should be accompanied by a steep rise in  $\tau$ .

The ESR spectral patterns of all the samples studied (Fig. 6) are indicative of a fast ( $\tau \leq 3 \times 10^{-9}$  s) anisotropic rotation of the spin label in the system. As the concentration of the  $\text{Sal}^-$  ions is increased up to about 0.05 M, the  $\tau$  values increase, and beyond this point the mobility of the label remains unchanged (Fig. 5). The increase in the  $\tau$  values, in our opinion, reflects the process of micelle elongation and growing proportion of surfactant **II** molecules packed more closely in cylindrical parts of the micelles than in their hemispherical ends. Beyond a certain concentration of counterions, the micelles become so oblong that the share of cylindrical portions is significantly higher than that of spherical ones, thus resulting in constant  $\tau$  values.

Thus, the NMR and ESR spectral data point to structural rearrangement in the studied micellar solutions of compound **II** at the NaSal concentration of about 0.05 M. It is readily seen from a comparison of Figs. 3 and 5 that the critical concentrations of the  $\text{Sal}^-$  ions fall in the region of sharp structural transformations of surfactant **II** micelles, implying a cause-and-effect relationship.

To conclude, the joint study of the kinetics of alkaline hydrolysis of phosphonic esters in micellar solutions of surfactant **II** and the structural parameters of the aggregates revealed the effect of electrolyte-induced structural rearrangements of surfactant **II** micelles on the reactivity of the esters.

## EXPERIMENTAL

The surface tension was determined by the anchoring method on Due-Nui tensiometer at 20°C [20].

The self-diffusion coefficients of components of micellar solutions were measured by  $^1\text{H}$  NMR spectroscopy with Fourier transform and pulse magnetic

field gradient on a Tesla BS-576A high-resolution spectrometer (100 MHz) [21].

The ESR spectra were recorded on an RE-1306 spectrometer in the conditions described in [22]. The spin label was 5-doxylstearic acid (Sigma,  $5 \times 10^{-4}$  M).

The kinetics of hydrolysis were studied spectrophotometrically on a Specord M-400 instrument at 25°C, following the absorbance of the *p*-nitrophenolate anion at  $\lambda$  400 nm. The initial concentration of the substrate in the kinetic experiments was  $5 \times 10^{-5}$  M. The apparent pseudo-first order rate constants ( $k_{\text{app}}$ ) were found from the equation  $\ln(A_{\infty} - A) = -k_{\text{app}}\tau + \text{const}$  ( $A$  and  $A_{\infty}$  are the optical densities of the solution at time  $\tau$  and on the completion of the reaction, respectively). The  $k_{\text{app}}$  values were calculated by the weighted least-squared method.

Ethyl *p*-nitrophenyl chloromethylphosphonate (**I**) and hexyl *p*-nitrophenyl chloromethylphosphonate (**III**) were prepared by the procedure described in [23]. Pure grade dodecylpyridinium bromide (surfactant **II**) was twice recrystallized from ethanol.

## ACKNOWLEDGMENTS

The work was financially supported by the Russian Foundation for Basic Research (project no. 99-03-32037a) and the Haldor Topse AG Company.

## REFERENCES

1. *Reaction Kinetics in Micelles*, Cordes, E.N., Ed., New York: Plenum, 1973, pp. 73–97.
2. *Surfactants in Solution*, Mittal, K.L., Ed., New York: Plenum, 1984, vol. 4, pp. 1015–1068.
3. Bunton, C.A., Nome, F., Quina, F.N., and Romsted, L.S., *Acc. Chem. Res.*, 1991, vol. 24, no. 12, pp. 357–364.
4. *Surfactants in Solution*, Mittal, K.L., Ed., New York: Plenum, 1984, vol. 3, pp. 825–840.
5. *Surfactants in Solution*, Mittal, K.L., Ed., New York: Plenum, 1984, vol. 2, pp. 805–824.
6. Shinoda, K., Nakagawa, T., Tamamushi, B.-I., and Isemura, T., *Colloidal Surfactants, Some Physicochemical Properties*, New York: Academic, 1963. Translated under the title *Kolloidnye poverkhnostno-aktivnye veshchestva*, Moscow: Mir, 1966, p. 319.
7. Zakharova, L.Ya., Fedorov, S.B., Kudryavtseva, L.A., Bel'skii, V.E., and Ivanov, B.E., *Izv. Ross. Akad. Nauk, Ser. Khim.*, 1993, no. 8, pp. 1396–1400.
8. Zakharova, L.Ya., Kudryavtseva, L.A., and Kononov, A.I., *Mendeleev Commun.*, 1998, vol. 8, no. 4, pp. 163–165.
9. *Micellization, Solubilization, and Microemulsions*, Mittal, K.L., Ed., New York: Plenum, 1977, vol. 2, pp. 489–507.
10. Shagidullina, R.A., Zakharova, L.Ya., and Kudryavtseva, L.A., *Izv. Ross. Akad. Nauk, Ser. Khim.*, 1999, no. 2, pp. 279–282.
11. Zakharova, L.Y., Valeeva, F.G., Kudryavtseva, L.A., and Kononov, A.I., *Mendeleev Commun.*, 2000, vol. 10, no. 6, pp. 241–243.
12. Rusanov, A.I. and Fainerman, V.B., *Dokl. Akad. Nauk SSSR*, 1989, vol. 308, no. 3, pp. 651–654.
13. Hobson, R.A., Grieser, F., and Healy, T.W., *J. Phys. Chem.*, 1994, vol. 98, no. 1, pp. 274–278.
14. Imae, T. and Koshaka, T., *J. Phys. Chem.*, 1992, vol. 96, no. 24, pp. 10030–10035.
15. Cassidi, M.A. and Warr, G.G., *J. Phys. Chem.*, 1996, vol. 100, no. 8, pp. 3237–3240.
16. Magid, L.J., Han, Z., Warr, G.G., Cassidi, M.A., Bulter, P.B., and Hamilton, W.A., *J. Phys. Chem. B*, 1997, vol. 101, no. 40, pp. 7919–7927.
17. Fedotov, V.D., Zuev, Yu.F., Archipov, V.P., and Idiyatullin, Z.Sh., *Appl. Magn. Reson.*, 1996, vol. 11, no. 1, pp. 7–17.
18. *Micellization, Solubilization, and Microemulsions*, Mittal K.L., Ed., New York: Plenum, 1977, vol. 1, pp. 359–381.
19. Tsvetkov, V.N., Eskin, V.E., and Frenkel', S.Ya., *Struktura makromolekul v rastvorakh* (Structure of Macromolecules in Solutions), Moscow: Nauka, 1964, p. 720.
20. Baranova, V.I., Bibik, E.E., Kozhevnikov, N.M., Larov, I.S., and Malov, V.A., *Praktikum po kolloidnoi khimii* (Laboratory Manual on Colloid Chemistry), Moscow: Vysshaya Shkola, 1983, p. 215.
21. Fedotov, V.D., Zuev, Yu.F., Archipov, V.P., Idiyatullin, Z.Sh., and Garti, N., *Colloids Surfaces*, 1997, vol. 128, no. 1, pp. 39–46.
22. Fedotov, V.D., Vylegzhanina, N.N., Altshuler, A.E., Shlenkin, V.I., Zuev, Yu.F., and Garti, N., *Appl. Magn. Reson.*, 1998, vol. 14, no. 3, pp. 497–512.
23. Bel'skii, V.E., Kudryavtseva, L.A., Il'ina, O.M., and Ivanov, B. E., *Zh. Obshch. Khim.*, 1970, vol. 49, no. 11, pp. 2470–2473.